Lateral torsional buckling of glulam beam-columns: Axial compression and bending verification

Janusch Töpler, Institute for Timber Design, Biberach University of Applied Sciences, Germany

Ulrike Kuhlmann, Institute of Structural Design, University of Stuttgart, Germany

Jörg Schänzlin, Institute for Timber Design, Biberach University of Applied Sciences, Germany

1 Introduction

Lateral torsional buckling (LTB) and subsequent member failure is a realistic risk for glulam (GL) beam-columns and represents a complex 3-dimensional mechanical behaviour, see Figure 1. Beam-columns can be designed according to EN 1995-1-1 (2004) and prEN 1995-1-1 (2024) by the simplified k_c-k_m-method or by calculation of internal forces according to 2nd order theory (T2O; subscript 2 in equations), see Figure 2. The current drawbacks of the k_c-k_m-method are: (i) the main part of the design equation of the k_m-method is a pure regression model that is not fully considering all relevant parameters; (ii) the mechanical background of the exponent 2 of the bending component of the

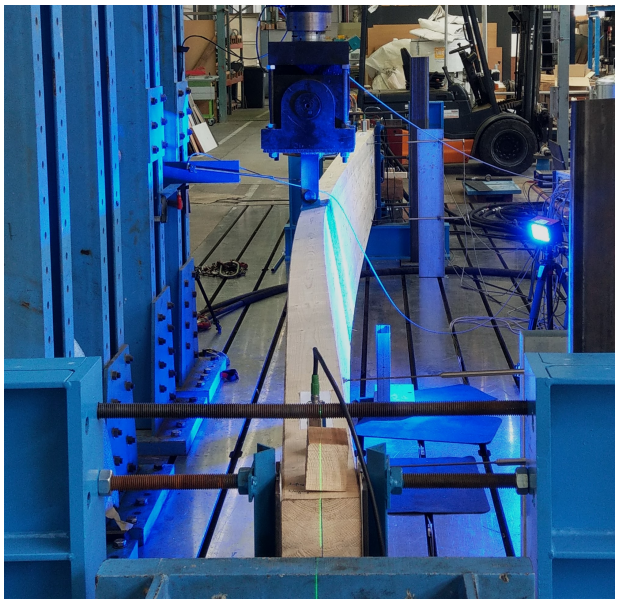

Figure 1. Lateral torsional buckling of a GL 24h beam-column with 600 · 120 · 8000 mm³.

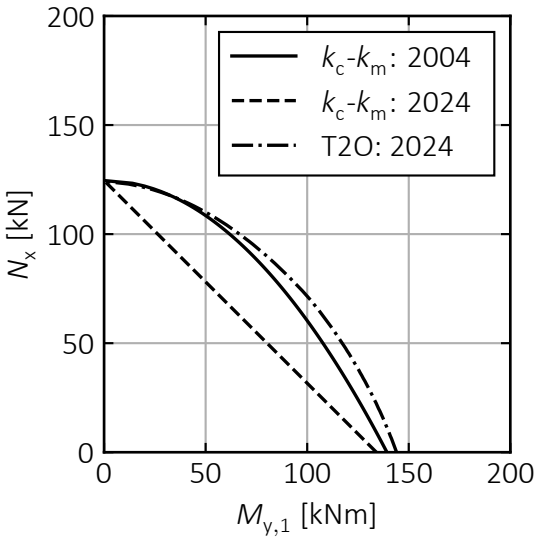

Figure 2. Load-bearing capacity of a GL 24h beam-column with 600 · 120 · 8000 mm³; k_c- k_m-method and design with T2O calculations from EN 1995-1-1 (2004) and prEN 1995-1-1 (2024).

N_x-$M_{y,1}$-interaction in EN 1995-1-1 (2004) was unclear during its revision and therefore a conservative linear interaction was reintroduced; (iii) the inconsistent imperfection assumptions discussed by *Töpler* & *Kuhlmann* (2023); and (iv) there were no results of LTB tests on GL beam-columns for validating the design equations.

This paper discusses the analytical background of the nonlinear N_x-$M_{y,1}$-interaction of the k_c-k_m-method and a mechanical derivation of new equations for the k_m-method. The results of 16 full-scale LTB tests on GL beam-columns are presented, which served as validation for a numerical model. An extensive numerical parameter study was conducted to investigate the influence of different loading scenarios, cross-sectional dimensions, and material grades on the N_x-$M_{y,1}$-interaction of timber beam-columns. The findings are compared with current design rules and literature. Finally, a proposal for a modification of the k_c-k_m-method and the design with internal forces according to T2O is presented, which increases reliability and allows for a more economic design.

The design for bending and axial compression is addressed in this article. A detailed report on the investigations is given by *Töpler* & *Kuhlmann* (2024) and *Töpler* (2025).

2 Design methods in Eurocode 5

2.1 Methods according to EN 1995-1-1 (2004)

In case of a geometrically nonlinear calculation of internal forces, e.g., by T2O, the LTB design with bending and compression can be carried out using Equations (1) and (2).

$$\left(\frac{\sigma_{c,0,d}}{f_{c,0,d}}\right)^2 + \frac{\sigma_{m,y,d}}{f_{m,y,d}} + k_{red} \cdot \frac{\sigma_{m,z,d}}{f_{m,z,d}} \leq 1.0 \tag{1}$$

$$\left(\frac{\sigma_{c,0,d}}{f_{c,0,d}}\right)^2 + k_{red} \cdot \frac{\sigma_{m,y,d}}{f_{m,y,d}} + \frac{\sigma_{m,z,d}}{f_{m,z,d}} \leq 1.0 \tag{2}$$

For rectangular cross-sections, the size effect on the bending strength at biaxial bending can be taken into account with $k_{red} = 0.7$, according to *Buchanan* et al. (1985) and *van der Put* (1991). The positive influence of compressive plasticizing on the cross-sectional resistance is taken into account by the exponent 2 at the compressive force component, which was derived by *Blaß* (1987), *Buchanan* et al. (1985), and *Zahn* (1986).

In case of a geometrically linear calculation of internal forces, by 1st order theory (T1O; subscript 1 in equations), the LTB design can be conducted with Equation (3).

$$\frac{\sigma_{c,0,d}}{k_{c,z} f_{c,0,d}} + \left(\frac{\sigma_{m,y,d}}{k_m f_{m,y,d}}\right)^2 \leq 1.0 \tag{3}$$

$k_{c,z}$ is based on the investigations by *Blaß* (1987), where the effects of geometrical bow imperfections, structural imperfections, and materially nonlinear behaviour (compressive

plasticizing in grain direction) are covered by β_c. The exponent 2 corresponds to the nonlinear interaction of $N_{z,crit}$ and $M_{y,crit}$ when determining the critical load, as suggested by *Leicester* (1988a) and discussed in Section 3.3. k_m can be calculated for $0.75 < \lambda_{m,rel} \leq 1.4$ as proposed by *Heimeshoff* (1986) with Equation (4).

$$k_m = 1.56 - 0.75\,\lambda_{m,rel} \tag{4}$$

Equation (4) is a regression model without mechanical background, which only partially covers the influence of the height-to-width ratio, material properties, and imperfections.

2.2 Methods according to prEN 1995-1-1 (2024)

In case of a geometrically nonlinear calculation of internal forces, e.g., by T2O, the LTB design with bending and compression can be carried out using Equations (1) and (2).

In case of a geometrically linear calculation of internal forces, by T1O, some modifications were made compared to EN 1995-1-1 (2004). As the mechanical background of the exponent 2 in Equation (3) was unclear during the revision of Eurocode 5, the linear N_x-$M_{y,1}$-interaction from, e.g., DIN 1052 (2004) was reintroduced, see Equation (5).

$$\frac{\sigma_{c,0,d}}{k_{c,z}\,f_{c,0,d}} + \frac{\sigma_{m,y,d}}{k_m\,f_{m,y,d}} \leq 1.0 \tag{5}$$

Equation (5) is significantly more conservative than Equation (3), see Figure 2. The k_c-method remained unchanged, but Equation (6) for calculating β_c was introduced.

$$\beta_{c,y/z} = \frac{e_{z/y}}{L} \cdot \pi \cdot \sqrt{\frac{3\,E_{0,k}}{f_{c,0,k}}} \cdot \frac{f_{c,0,k}}{f_{m,y/z,k}} \tag{6}$$

where $e_{y/z}$ is the equivalent bow imperfection, L is the member length, and $E_{0,k}$, $f_{c,0,k}$, and $f_{m,y/z,k}$ are the characteristic values of the elastic modulus and strengths. Equation (6) was derived from the differential equations for in-plane buckling with linear N_x-$M_{y,2}$-interaction, see *Schänzlin* et al. (2022). In contrast to the β_c values given in EN 1995-1-1 (2004), no positive or negative effect of compressive plasticizing in grain direction is taken into account in Equation (6). k_m can be calculated with Equations (7) and (8).

$$k_m = \frac{1}{\Phi_m + \sqrt{\Phi_m^2 - \lambda_{m,rel}^2}} \tag{7}$$

$$\Phi_m = 0.5 \cdot \left(1 + \beta_\Theta + \beta_m \cdot (\lambda_{m,rel} - 0.55) + \lambda_{m,rel}^2\right) \tag{8}$$

β_Θ and β_m can be determined according to prEN 1995-1-1 (2024) similarly to β_c. Equations (7) and (8) were shaped to resemble the k_c-method and are still based on a regression model without mechanical background.

3 Analytical background

3.1 General

This section contains the analytical background of the interaction equations in EN 1995-1-1 (2004), see Equations (1), (2), and (3), and a mechanically sound analytical derivation of new equations for the k_m-method. Most was already discussed by other authors, but sometimes in a different or more complex shape, and some so far back in time that they might not be remembered anymore. Further details are given by *Töpler* (2025).

3.2 Exponent 2 at the compressive force component

A model presented by *van der Put* (1991) is employed in this paper to analytically derive an N_x-$M_{y,2}$-interaction relationship that incorporates plasticizing and to validate the exponent 2 in Equations (1) and (2).

For a bilinear elastoplastic material behaviour in grain direction and the stress distribution in Figure 3, the axial compressive force N_x and the bending moment $M_{y,2}$ can be calculated with Equations (9) and (10) according to *van der Put* (1991).

$$N_x = f_{c,0}\, H\, B + \frac{f_m - f_{c,0}}{2} \cdot (H - H_{pl}) \cdot B \tag{9}$$

$$M_{y,2} = \frac{f_m - f_{c,0}}{2} \cdot (H - H_{pl}) \cdot \left(\frac{H}{2} - \frac{H - H_{pl}}{3}\right) \cdot B \tag{10}$$

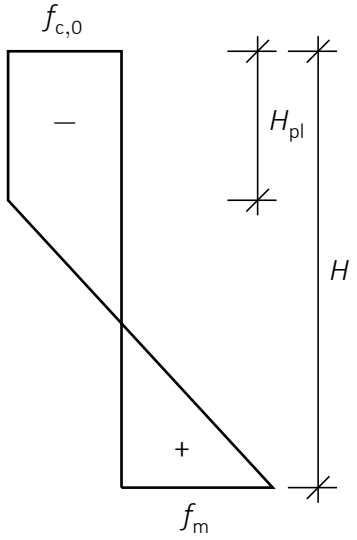

Figure 3. Distribution of stresses in grain direction over the cross-sectional height H for a combined loading by an axial compressive force N_x and a bending moment $M_{y,2}$ with bilinear elastoplastic material behaviour.

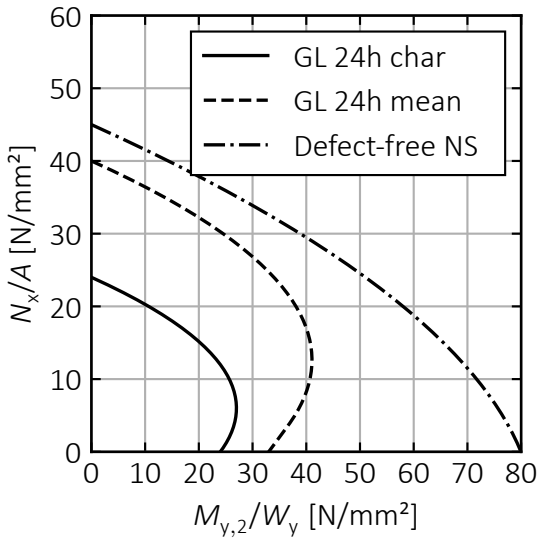

Figure 4. Cross-sectional resistances for a combined loading by an axial compressive force N_x and a bending moment $M_{y,2}$ and bilinear elastoplastic material behaviour for three timber materials with different $f_{c,0}$ and f_m.

where $f_{c,0}$ is the compressive strength (only in Section 3.2 with the mechanically correct negative sign), f_m is the bending strength, H and B are the cross-sectional height and width, and H_{pl} is the height of the plastic area. Solving Equation (9) for H_{pl} and inserting the result in Equation (10) leads, after some transformations, to the familiar-looking interaction in Equation (11) with Equations (12) and (13).

$$\left(\frac{N_x}{A f_{c,0}}\right)^2 - a \cdot \frac{N_x}{A f_{c,0}} + \frac{M_{y,2}}{W_y f_m} = b \tag{11}$$

$$a = \left(\frac{5 f_{c,0}^2 + 3 f_{c,0} f_m}{f_m^2 - f_{c,0} f_m} - \frac{4 f_{c,0}^2 - f_m^2 + f_{c,0} f_m}{f_m^2 - f_{c,0} f_m} \cdot \frac{N_x}{A f_{c,0}}\right) \tag{12}$$

$$b = \frac{-3 f_{c,0} f_m - f_{c,0}^2}{f_m^2 - f_{c,0} f_m} \tag{13}$$

where A is the cross-sectional area and W_y is the elastic section modulus. The interaction equation thus depends on the ratio of $f_{c,0}/f_m$.

Table 1 provides the values of a and b and the resulting interaction equations, and Figure 4 illustrates three cases. Figure 4 demonstrates the high impact of the $f_{c,0}/f_m$ ratio on the nonlinearity of the N_x-$M_{y,2}$-interaction relationship. For common values of $f_{c,0,k}$ and $f_{m,k}$, the parameters a and b become $a > 0$ and $b \approx 1$, see Table 1. Therefore, a can be neglected on the safe side (greyed out in Table 1). This results in Equation (14) which is identical to Equation (1) from EN 1995-1-1 (2004) and prEN 1995-1-1 (2024), except for the additional $M_{z,2}$ component in the standards.

$$\left(\frac{N_x}{A f_{c,0}}\right)^2 + \frac{M_{y,2}}{W_y f_m} = 1 \tag{14}$$

This interaction formula is therefore a mechanically sound limit criterion for tensile failure due to combined axial compression and bending, considering compressive plasticizing.

Table 1. Values of a and b and interaction equations for different timber materials with the compressive utilisation ratio $\mu_c = N_x/A f_{c,0}$ and the bending utilisation ratio $\mu_m = M_{y,2}/W_y f_m$.

	$f_{c,0}/f_m$ [1] [N/mm²]	a $\mu_c = (0, 0.5, 1)$	b	Interaction equation
GL 24c char [2]	-21.0 / 24.0	(0.62, 0.31, 0.01)	0.99	$\mu_c^2 - \mu_c(0.62 - 0.61\mu_c) + \mu_m = 0.99$
GL 24h char [2]	-24.0 / 24.0	(1.00, 0.50, 0.00)	1.00	$\mu_c^2 - \mu_c(1.00 - 1.00\mu_c) + \mu_m = 1.00$
GL 30c char [2]	-24.5 / 30.0	(0.44, 0.23, 0.02)	0.98	$\mu_c^2 - \mu_c(0.44 - 0.42\mu_c) + \mu_m = 0.98$
GL75 char [3]	-59.4 / 75.0	(0.36, 0.20, 0.03)	0.97	$\mu_c^2 - \mu_c(0.36 - 0.33\mu_c) + \mu_m = 0.97$
GL 24h mean [4]	-40.0 / 33.0	(1.68, 0.85, 0.02)	0.98	$\mu_c^2 - \mu_c(1.68 - 1.66\mu_c) + \mu_m = 0.98$
Defect-free NS [5]	-45.0 / 80.0	(-0.24,-0.01, 0.22)	0.78	$\mu_c^2 + \mu_c(0.24 - 0.46\mu_c) + \mu_m = 0.78$

[1] If $-f_{c,0} < f_m$, the input bending strength for Equations (11) to (13) need to be chosen higher than f_m for actually reaching the bending resistance $f_m W_y$ due to the plasticizing.

[2] EN 14080 (2013); [3] ETA-14/0354 (2018); [4] *Schilling* et al. (2021); [5] Norway spruce (NS) DIN 68364 (2003).

3.3 Nonlinear N_x-$M_{y,1}$-interaction for lateral torsional buckling

Leicester (1988a) demonstrated that the N_x-$M_{y,1}$-interaction for LTB is nonlinear. The derivation is given below.

For LTB of beam-columns, the critical load is given by Equation (15), see *Hörsting* (2008).

$$\alpha_{c,z} + \alpha_m^2 = 1 \tag{15}$$

where $\alpha_{c,z} = N_x/N_{z,crit}$, $\alpha_m = M_{y,1}/M_{y,crit}$, $N_{z,crit}$ is the critical compressive load for in-plane buckling around the z axis, and $M_{y,crit}$ is the critical bending moment for LTB.

Additionally, for very slender beam-columns, the member resistances approach the critical loads and $k_{c,z}\, A\, f_{c,0} \rightarrow N_{z,crit}$ and $k_m\, W_y\, f_m \rightarrow M_{y,crit}$, where $k_{c,z}$ and k_m are the reduction factors from the k_c- and the k_m-method, A is the cross-sectional area, W_y is the elastic section modulus, $f_{c,0}$ is the compressive strength, and f_m is the bending strength. Thus, Equation (15) can be rearranged to Equation (16), which is identical to the N_x-$M_{y,1}$-interaction for LTB in EN 1995-1-1 (2004), see Equation (3).

$$\frac{N_x}{k_{c,z}\, A\, f_{c,0}} + \left(\frac{M_{y,1}}{k_m\, W_y\, f_m}\right)^2 \rightarrow 1 \tag{16}$$

No size effect must be applied to f_m in this interaction, as it describes the critical load of very slender beam-columns, which is purely stiffness-dependent.

3.4 Reduction factor k_m accounting for lateral torsional buckling

Leicester (1988b), *Taras* (2010), and *Wilden* et al. (2023) discussed a mechanically sound derivation of the reduction factor k_m that accounts for LTB. The derivation is given below. For timber construction, the formulation with bow imperfections e_y instead of twist imperfections e_Θ in Equation (25) is new.

The differential equations for LTB with a constant bending moment $M_{y,1}$, see e.g., *Hörsting* (2008), are the basis of the derivations. By means of the initial functions $v_2(x) = v_2 \cdot \sin(\pi \cdot x/L)$ and $\Theta_2(x) = \Theta_2 \cdot \sin(\pi \cdot x/L)$, the differential equations can be transformed into Equations (17) and (18), which are valid at midspan.

$$G_0\, I_x\, \Theta_2 - M_{y,1} \cdot (v_2 + e_y) = 0 \tag{17}$$

$$\frac{\pi^2}{L^2}\, E_0\, I_z\, v_2 - M_{y,1} \cdot (\Theta_2 + e_\Theta) = 0 \tag{18}$$

where G_0 and E_0 are the shear and elastic moduli in grain direction, I_x and I_z are the respective moments of inertia, v_2 and Θ_2 are the deformation in y direction and the rotation around the x axis at midspan, e_y and e_Θ are the bow imperfection in y direction and the twist imperfection at midspan, and L is the member length.

The key in the derivation is the assumption that the imperfections are affine to the 1st eigenmode, $e_y = k v_2$ and $e_\Theta = k \Theta_2$, where k is a scaling factor. Inserting this into Equations (17) and (18) and then inserting Equations (17) in (18) results after a few transformations in Equation (19).

$$\frac{e_y}{e_\Theta} = \frac{M_{y,crit}}{N_{z,crit}} \tag{19}$$

A linear $M_{y,2}$-$M_{z,2}$-interaction according to Equation (20) is assumed.

$$\frac{M_{y,2}}{W_y f_m} + \frac{M_{z,2}}{W_z f_m} = 1 \tag{20}$$

$M_{z,2}$ can be calculated with Equation (21) according to prEN 1995-1-1 (2024).

$$M_{z,2} = \frac{\frac{M_{y,1}^2}{G_0 I_x} e_y + M_{y,1}\, e_\Theta}{1 - \alpha_m^2} \tag{21}$$

With the coupled imperfections from Equation (19), Equation (21) can be simplified to Equation (22).

$$M_{z,2} = \frac{\alpha_m\, N_{z,crit}\, e_y}{1 - \alpha_m} \tag{22}$$

The common assumption is made that the geometrically nonlinear LTB behaviour does not significantly influence the bending moment around the strong axis, and $M_{y,2} = M_{y,1}$ applies. Inserting $M_{y,2}$ and $M_{z,2}$ in Equation (20) leads to a quadratic equation that can be solved in a similar way to the k_c-method, which results in Equations (23) to (25).

$$k_m = \frac{1}{\Phi_m + \sqrt{\Phi_m^2 - \lambda_{m,rel}^2}} \tag{23}$$

$$\Phi_m = 0.5 \cdot \left(1 + \beta_m + \lambda_{m,rel}^2\right) \tag{24}$$

$$\beta_m = \frac{e_y}{L} \cdot \frac{H}{B} \cdot \frac{\pi}{2} \cdot \sqrt{\frac{E_0}{G_0}} \tag{25}$$

Equations (23) to (25) are similar to the k_m-method in prEN 1995-1-1 (2024), see Equations (7) and (8), except for the lack of the β_Θ and the $(\lambda_{m,rel} - 0.55)$ components. The advantage of Equations (23) to (25) is the discussed mechanical background that Equations (4), (7), and (8) are lacking.

4 Experiments

4.1 General

16 LTB tests with combined axial compression and bending on GL 24h according to EN 14080 (2013) were conducted within the research project IGF 21285 N, see *Töpler* & *Kuhlmann* (2024). Two parameters were varied: the slenderness ratio $\lambda_{m,rel}$ by means of the member length and height, and the utilisation ratio $\mu_c = N_x/N_{x,R}$ of the axial compressive resistance, calculated with the k_c-method in EN 1995-1-1 (2004), see Table 2. A more detailed description of the LTB tests is given in *Töpler* & *Kuhlmann* (2023).

Table 2. Test program for lateral torsional buckling of glulam GL 24h beams.

Series number	Number of specimens	Length [mm]	Height x Width [mm^2]	$\lambda_{m,rel}$ [1]	μ_c	N_x [kN]
T04 – T05	2	8000	600 x 120	0.94	0.00	0
T06 – T07	2	8000	600 x 120	0.94	0.20	25
T08 – T09	2	8000	600 x 120	0.94	0.40	50
T10 – T11	2	8000	600 x 120	0.94	0.60	75
T12 – T13	2	6000	480 x 120	0.74	0.00	0
T14 – T15	2	6000	480 x 120	0.74	0.20	35
T16 – T17	2	6000	480 x 120	0.74	0.40	70
T18 – T19	2	6000	480 x 120	0.74	0.60	105

[1] Calculated with characteristic material values, taking into account an increase of $E_{0,05}G_{0,05}$ by a factor of 1.4 according to DIN EN 1995-1-1/NA (2013).

4.2 Test setup and execution

At one end of the beams, at the front in Figure 1, the horizontal support was formed by an abutment and a centrally located calotte. At the other end, at the rear in Figure 1, the horizontal load was applied centrally by a cylinder with a yoke joint. Vertical loading, vertical supports, and measuring devices are described in *Töpler* & *Kuhlmann* (2023).

First, the axial compressive force was applied force-controlled up to the values given in Table 2. Secondly, the vertical force was applied displacement-controlled at midspan.

4.3 Results and evaluation

Typical load-deformation curves with the horizontal deformation of the beam axis at midspan v and the vertical cylinder force F_z are given in Figure 5. The general load-bearing behaviour is described in *Töpler* & *Kuhlmann* (2023). As the axial compressive force increased, (i) the peak of the load-deformation curve shifted to the left; (ii) the maximum vertical force F_z decreased; and (iii) the maximum deformations v increased.

The experimentally determined load-bearing capacities are plotted in Figure 6, where $M_{y,1}$ is the bending moment applied by F_z. Additionally, the characteristic resistances from the k_c-k_m-method and design with calculations using T2O from EN 1995-1-1 (2004) and DIN EN 1995-1-1/NA (2013), and the results of FE analyses with the same input values are given. The FE model is described in Section 5. The bow imperfection was

chosen to be equal to the horizontal eccentricity of the vertical force. Experimentally, an increase in the compressive force and its utilisation ratio μ_c from 0% to 60% reduced the bending load-bearing capacity by about 20%. This confirmed the nonlinearity of the N_x-$M_{y,1}$-interaction curve of the k_c-k_m-method in EN 1995-1-1 (2004), see Equation (3) and was supported by the results of comparative calculations with T2O and FE analyses.

The failure behaviour is described in *Töpler* & *Kuhlmann* (2023). No influence of the axial compressive force on the failure mode was detected.

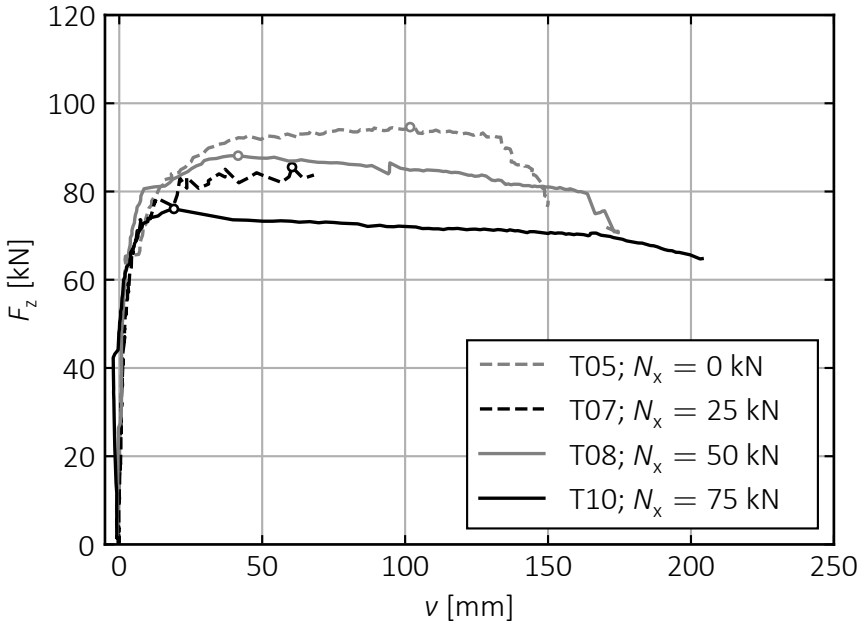

Figure 5. LTB tests T05, T07, T08, and T10 with $\lambda_{m,rel} = 0.94$; vertical force F_z plotted over the horizontal deformation of the beam axis at midspan v; circles mark maximum vertical forces.

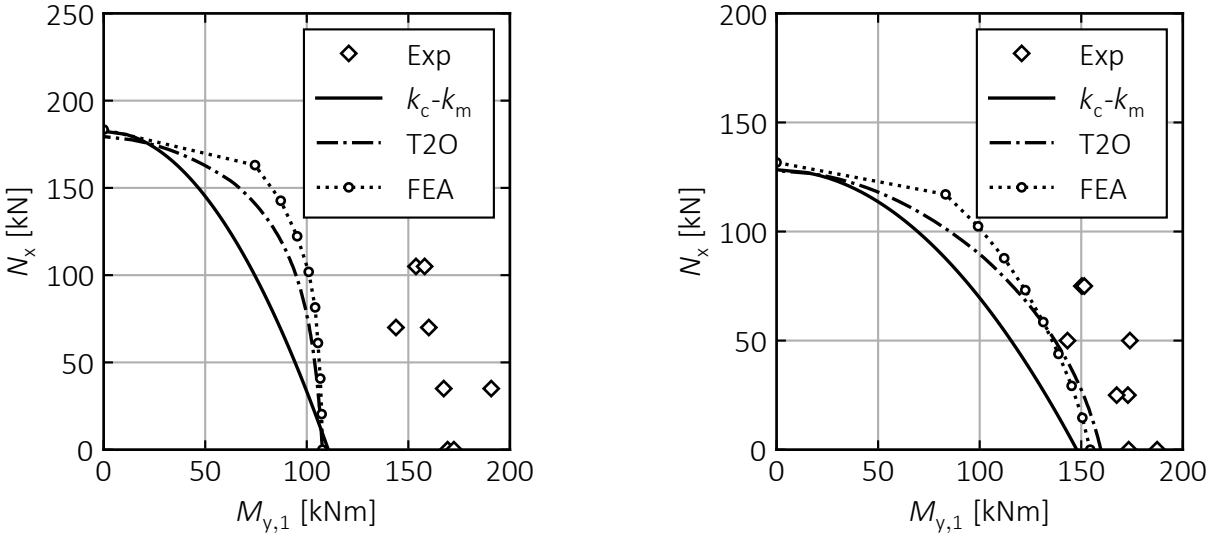

(a) 480 · 120 · 6000 *mm³.* *(b)* 600 · 120 · 8000 *mm³.*

Figure 6. Experimentally (Exp) determined load-bearing capacities; characteristic resistances of the k_c-k_m-method and design with calculations using T2O according to EN 1995-1-1 (2004) and DIN EN 1995-1-1/NA (2013); and characteristic resistances from FE analyses.

5 Numerical simulations

5.1 General

The numerical simulations were conducted for an in-depth analyses of the influence of the slenderness, the material, and the loading on the N_x-$M_{y,1}$-interaction curves for LTB with combined axial compression and bending. The numerical analyses were conducted with solid elements in Abaqus/CAE 2023. A description of the model and its verification and validation is given in *Töpler* & *Kuhlmann* (2023) and *Töpler* & *Kuhlmann* (2024).

Single-span beams with fork bearings were investigated, loaded by a constant bending moment, by a uniform line load at the upper edge of the beam, or by a concentrated load at midspan at the upper edge of the beam. In addition, the axial compressive force was varied. The axial compressive force was applied first and kept constant. Afterwards, the bending moment was applied. For the constant bending moment, an idealised support in the member axis was modelled. For the uniform line load or the concentrated load, a realistic support at the lower edge of the beam was created.
GL 24h, GL 30c, and GL75 with the nominal material properties and an anisotropic material model with elastoplastic behaviour for compression in grain direction and shear were analysed, see also *Töpler* & *Kuhlmann* (2023) and *Töpler* & *Kuhlmann* (2024). Shear was always neglected as a failure criterion in the evaluation of the FE analyses.
Equivalent bow and twist imperfections at midspan of $e_y = L/1000$ and $e_\Theta = 0.5 \cdot (e_{\Theta,\text{mid}} + e_{\Theta,\text{supp}})$ with $e_{\Theta,\text{supp}} = 1/100$ and $e_{\Theta,\text{supp}} = L/1500H$ were assumed according to the investigations in *Töpler* & *Kuhlmann* (2023). Cross-sectional height-to-width ratios of 1, 2, 4, 8, 12, and 16 were modelled with a width of 120 mm. The member length was varied between 2.5H and 25H or 50H. This resulted in over 17,000 FE analyses.

5.2 Results

5.2.1 Plate bending around the x axis

With an increasing height-to-width (H/B) ratio at the same relative slenderness $\lambda_{m,rel}$, the LTB deformation behaviour of the timber beams significantly changed, see Figure 7. At $H/B = 4$, no plate bending was observed. At $H/B = 12$, a strong plate bending around the x axis occurred, which increased the eigenvalues and the load-bearing capacities by up to 20% compared to calculations with beam theory. The effect was greatest for the constant bending moment. With an increasing H/B ratio, the ratio of the plate bending stiffness to the buckling stiffness of the compression chord decreases, and the deformation behaviour changes. With regard to this effect, calculations of eigenvalues and load-bearing capacities based on beam theory, e.g., the design equations in EN 1995-1-1 (2004), provide conservative results for beams with large H/B ratios.

The pronounced plate bending at large H/B ratios is characteristic of the anisotropic material timber, with its large difference between the elastic moduli in grain direction and perpendicular to the grain, the large E_0/E_{90} ratio. For isotropic materials such as steel and concrete, the effect can only be observed at significantly higher H/B ratios.

5.2.2 *Cross-sectional warping due to shear forces*

Figure 8 displays the reduction factors k_m calculated from the FE results over the relative LTB slenderness $\lambda_{m,rel}$ for different utilisation ratios of the axial compressive resistance μ_c for loading by a constant bending moment and by a concentrated force. $\lambda_{m,rel}$ was calculated using prEN 1995-1-1 (2024). Beams subjected to shear forces had significantly lower load-bearing capacities for $L/H < 6$. See the drop of k_m at $L/H < 6$ in Figure 8b in comparison with Figure 8a. This can be explained by the fact that shear stresses due to shear forces led to cross-sectional warping and its obstruction to residual stresses, secondary stresses, in grain direction. The superposition of these secondary stresses with the primary stresses from bending increased in the edge bending stresses and thus reduced the load-bearing capacities, see also *Töpler* & *Kuhlmann* (2022a).

The fact that this effect occurred for $3 < L/H < 6$ is characteristic of timber with its large difference between the elastic and shear moduli in grain direction, the large E_0/G_0 ratio.

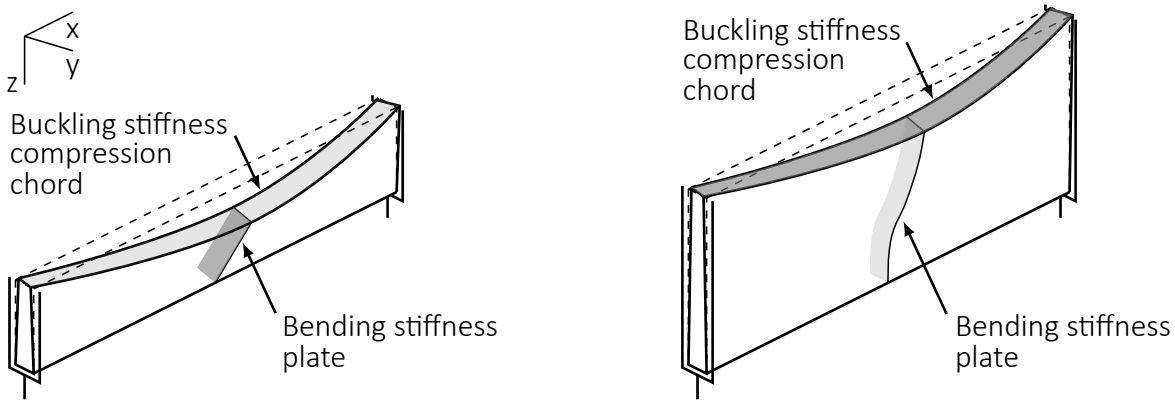

(a) $H/B = 4$. *(b) $H/B = 12$.*

Figure 7. Schematic illustration of lateral torsional buckling deformation behaviours of timber beams.

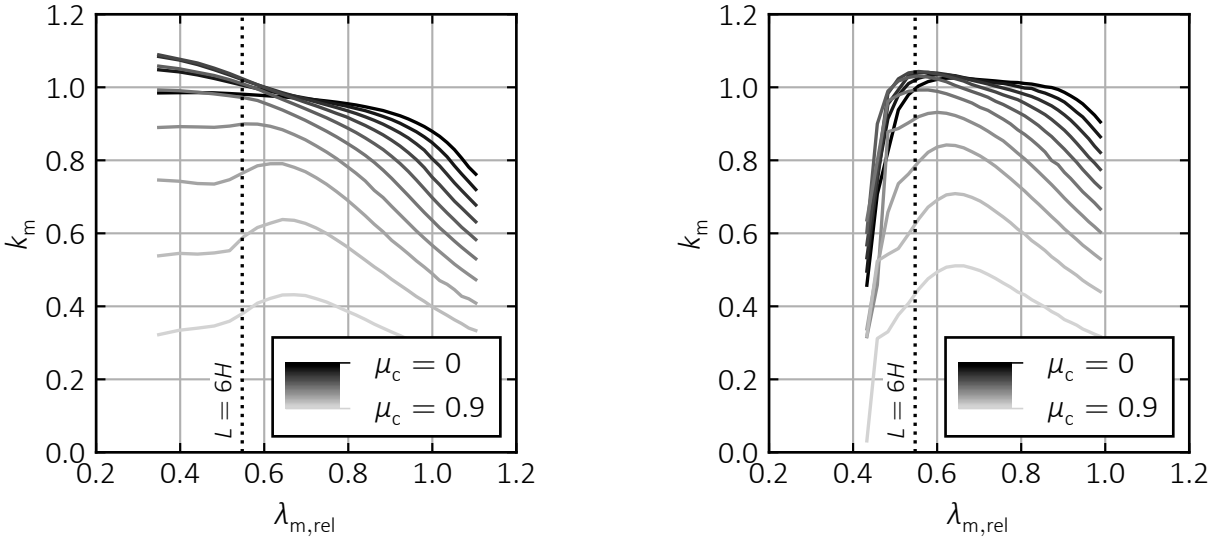

(a) Constant bending moment. *(b) Concentrated force at midspan.*

Figure 8. Reduction of the load-bearing capacity k_m from FE analyses over the relative LTB slenderness $\lambda_{m,rel}$ according to prEN 1995-1-1 (2024) for different utilisation ratios μ_c; GL 24h and $H/B = 4$.

5.2.3 N_x-$M_{y,1}$-interaction

At $\lambda_{m,rel} > 0.7$, the load-bearing capacities, or k_m, in Figure 8 followed the typical lateral-torsional buckling curves and decreased with increasing slenderness. With increasing compressive load, or μ_c, k_m decreased nonlinearly, first less, then more.
At $\lambda_{m,rel} < 0.7$, the influences of (i) shear warping, see Section 5.2.2, (ii) compressive plasticizing in grain direction, and (iii) the nonlinear interaction relationship of the critical load, see Equation (15), were overlapping. For beams subjected to shear forces, the influence of shear warping was decisive, and it significantly reduced the load-bearing capacity, see Figure 8b. For beams subjected to a constant bending moment, no shear warping occurred, see Figure 8a. Plasticizing even increased the bending load-bearing capacity for low compressive forces, $k_m > 1$, and decreased k_m nonlinearly for higher compressive forces, first less, then more. With increasing $\lambda_{m,rel}$, the influence of compressive plasticizing decreased, which tended to reduce the load-bearing capacity. This effect was overlapped by the increasing influence of the nonlinear interaction relationship of the critical load with increasing slenderness. Thus, for high utilisation ratios μ_c, despite decreasing compressive plasticizing, there was sometimes an increase in bending load-bearing capacity with a peak at $\lambda_{m,rel} \approx 0.5$ to 0.8.

In-plane buckling occurred for $H/B = 1$ and LTB for $H/B \geq 2$.

Figure 9 presents two typical N_x-$M_{y,1}$-interaction diagrams from FE analyses for two H/B ratios with varying relative in-plane buckling and LTB slendernesses $\lambda_{c,y,rel}$ and $\lambda_{m,rel}$. The relative load-bearing capacities are given as ratios of the bending or compressive load-bearing capacity to the load-bearing capacity for pure bending or pure compression (including stability behaviour). Additionally, for $H/B = 1$, the linear interaction is plotted,

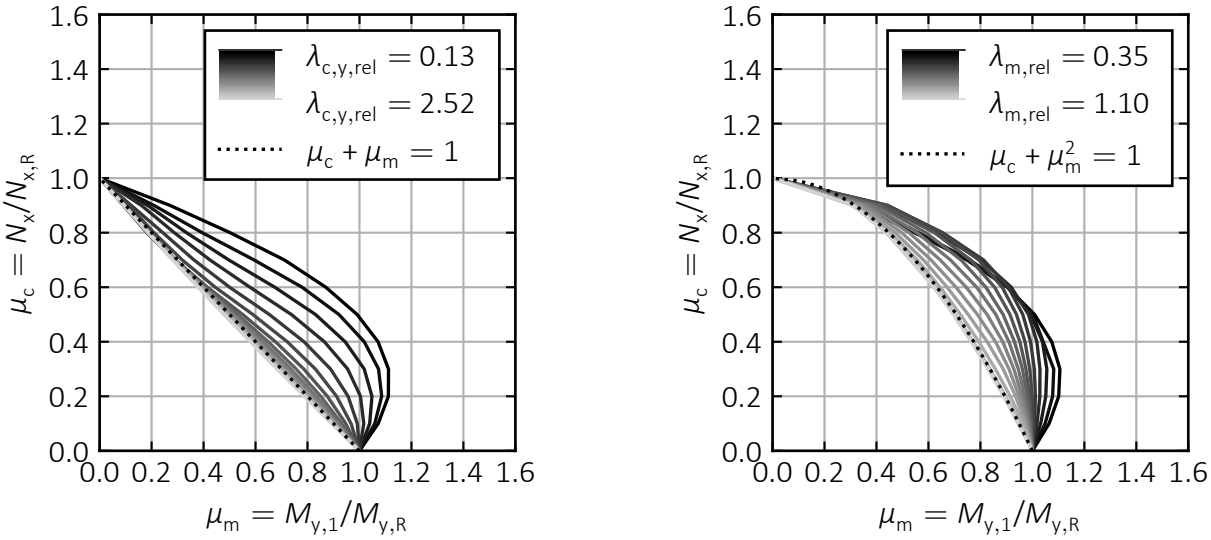

(a) $H/B = 1$ and varying $\lambda_{c,y,rel}$. *(b) $H/B = 4$ and varying $\lambda_{m,rel}$.*

Figure 9. Relative compressive load-bearing capacity $N_x/N_{x,R}$ over the relative bending load-bearing capacity $M_{y,1}/M_{y,R}$ from FE analyses; GL 24h and constant bending moment.

and for $H/B = 4$, the limit condition according to Equation (3) is plotted.
For $H/B = 1$, a distinctly nonlinear N_x-$M_{y,1}$-interaction occurred for $\lambda_{c,y,rel} \approx 0.3$, which was caused by compressive plasticizing in grain direction, see Figure 9a. With increasing slenderness, the non-linearity of the N_x-$M_{y,1}$-interaction decreased until it was almost linear for $\lambda_{c,y,rel} = 0.8$ (GL75) to 1.2 (GL 24h). For large slendernesses, the compressive forces were so small that no (significant) plasticizing occurred.
For $H/B \geq 2$, the N_x-$M_{y,1}$-interaction was always distinctly nonlinear, see Figure 9b. At low slendernesses, the same nonlinear curve as for $H/B = 1$ occurred as a result of compressive plasticizing. With increasing slenderness, there was a slight increase in non-linearity due to the superposition of the influence of compressive plasticizing and the nonlinear interaction relationship of the critical load, see Equation (15). Subsequently, the nonlinearity decreased and approached the limit value of the critical load from Equation (15), which was reached between $\lambda_{m,rel} = 0.8$ (GL75) and 0.9 (GL 24h). The load-bearing capacity of slender beams was equal to the critical load.

For significant shear forces, here induced by a concentrated force or a uniform line load, and $1.0 \leq \lambda_{m,rel} \leq 1.5$, a reduction in shear stiffness due to shear plasticizing occurred, which reduced the load-bearing capacity by up to 20%. This “shear plasticizing” due to local shear cracks was discussed by *Töpler* & *Kuhlmann* (2023).

For GL75, due to the high compressive plasticizing, see *Töpler* & *Kuhlmann* (2022b), larger stiffness reductions occurred than for GL 24h and GL 30c. This effect reduced the non-linearity of the N_x-$M_{y,1}$-interaction curve at low slendernesses compared to GL 24h in Figure 9.

6 Discussion

For in-plane buckling, $H/B \approx 1$, *Blaß* (1987), *Buchanan* et al. (1985), and *Zahn* (1986) reported similar results as the numerical results in Figure 9a, which yielded a linear N_x-$M_{y,1}$-interaction for slender members and a nonlinear N_x-$M_{y,1}$-interaction for stocky members. This is also reflected in the design procedures according to EN 1995-1-1 (2004) and prEN 1995-1-1 (2024), see Sections 2.1 and 2.2.

For LTB, $H/B \gtrapprox 2$, the analytical derivations, see Section 3.3, the experimental results, see Section 4.3, and the FE results, see Section 5.2.3, confirmed the non-linearity of the N_x-$M_{y,1}$-interaction for stocky and slender members. In addition to the analytical derivation of *Leicester* (1988b), see Section 3.3, *Bell* & *Eggen* (2001) presented numerical calculation results that produced a similar nonlinear interaction relationship. This is also reflected by the nonlinear Equation (3) from EN 1995-1-1 (2004), but not anymore by the conservative linear Equation (5) from prEN 1995-1-1 (2024).

The authors are not aware of any investigations concerning the influence of the plate bending at LTB of timber beams with large H/B ratios. Also, cross-sectional warping due to shear has not yet been reported, with the exception of the own investigations in *Töpler* & *Kuhlmann* (2022a).

7 Design proposals

For the k_c-k_m-method, it is highly recommended to reintroduce the nonlinear N_x-$M_{y,1}$-interaction from EN 1995-1-1 (2004), Equation (3), in prEN 1995-1-1 (2024) for an economic design of timber beam-columns.

For considering the material-dependent stiffness reduction due to compressive plasticizing at in-plane buckling and the shear force-dependent stiffness reduction due to shear plasticizing at LTB, it is proposed to introduce the coefficients $k_{pl,c}$ and $k_{pl,m}$ and to modify the formulas of T2O in prEN 1995-1-1 (2024), see Equations (26) to (28).

$$M_{x,2} = \frac{\pi}{L} \cdot \frac{M_{y,1}\, k_{pl,m}\, e_y + \alpha_m^2\, G_0\, I_x\, e_\Theta}{1 - \alpha_{c,z} - \alpha_m^2} \tag{26}$$

$$M_{y,2} = \frac{N_x\, k_{pl,c}\, e_z + M_{y,1} \cdot (1 + \alpha_{c,y}\delta_y)}{1 - \alpha_{c,y}} \tag{27}$$

$$M_{z,2} = \frac{\left(N_x k_{pl,c} + \frac{M_{y,1}^2}{G_0 I_x} \cdot k_{pl,m}\right) \cdot e_y + M_{y,1} e_\Theta + M_{z,1} \cdot (1 + \alpha_{c,z}\delta_z)}{1 - \alpha_{c,z} - \alpha_m^2} \tag{28}$$

For the k_c- and the k_m-method, it is proposed to include $k_{pl,c}$ and $k_{pl,m}$ in the calculation of β_c and β_m by Equations (29) and (30).

$$\beta_{c,y/z} = k_{pl,c} \cdot \frac{e_{z/y}}{L} \cdot \pi \cdot \sqrt{\frac{3E_{0,k}}{f_{c,0,k}}} \cdot \frac{f_{c,0,k}}{f_{m,y/z,k}} \tag{29}$$

$$\beta_m = k_{pl,m} \cdot \frac{e_y}{L} \cdot \frac{H}{B} \cdot \frac{\pi}{2} \cdot \sqrt{\frac{E_{0,k}}{G_{0,k}}} \tag{30}$$

For softwood GL and LVL, $\beta_c = 0.1$, and $\beta_m = 0.01 \cdot k_{pl,m} \cdot H/B$ and for solid timber made of softwood, $\beta_c = 0.2$ and $\beta_m = 0.02 \cdot k_{pl,m} \cdot H/B$ may be used.
$k_{pl,c}$ and $k_{pl,m}$ were determined by curve fitting of Equations (26) to (28) to the FE results, see *Töpler & Kuhlmann* (2024). For softwood, $k_{pl,c} = 1$ should be assumed. For beech, a value of $k_{pl,c} \approx 4$ at $e_{y/z} = L/1000$ is plausible, see *Töpler & Kuhlmann* (2022b). For softwood without significant shear forces, $k_{pl,m} = 1$ and with significant shear forces, $k_{pl,m} = 6$ should be assumed. Further research on determining $k_{pl,c}$ for wood species other than softwood and specifying $k_{pl,m}$ for shear forces is required.

For the k_m-method, it is proposed to apply the mechanically derived Equations (23) and (24). Additionally, a limit value can be introduced for design practice, above which $k_m < 1.0$, i.e. LTB, should be taken into account, see Equation (31).

$$\Phi_m = 0.5 \cdot \left(1 + \beta_m \cdot (\lambda_{m,rel} - 0.7) + \lambda_{m,rel}^2\right) \tag{31}$$

The limit criterion 0.7 was determined based on the point where $k_m = 0.9$ in calculations using T2O, see *Töpler & Kuhlmann* (2024).

For considering the increase in edge bending stresses due to cross-sectional warping, it is recommended to introduce a respective clause in prEN 1995-1-1 (2024):
(x) The increase in edge bending stresses due to shear-induced cross-sectional warping should be taken into account for members with significant bending and shear stresses in the same plane and $L/H < 6$. This may be done by analyses with membrane theory.
Simplified formulas for considering the increase in bending stress could be determined by further experimental and numerical investigations.

Figures 10a and 10b exemplary present the ratio of the reduction factors by the k_c-k_m-method and by calculations using T2O with the proposed changes to results from FE analyses, $k_{m,prop}/k_{m,FEA}$, over $\lambda_{m,rel}$ for GL 24h, $H/B = 8$, and a constant bending moment or a concentrated force at midspan. For $\lambda_{m,rel} > 1.2$, the load-bearing capacities according to the design methods and FE analyses are very similar. Minor deviations for concentrated forces and high μ_c result from the general application of $k_{pl,m}$, although shear plasticizing decreases with increasing μ_c. For $\lambda_{m,rel} < 1.2$ and constant bending moment, the k_c-k_m-method is clearly on the safe side at high μ_c, as the positive effects of compression plasticizing are not fully considered. For $\lambda_{m,rel} < 1.2$ and concentrated forces, the importance of the limiting criterion $L/H \geq 6$ for the application of the beam theory is demonstrated. Both the limit criterion $L/H \geq 6$ and $k_{pl,m}$ could be formulated in more detail to take into account the influence of the utilisation ratio μ_c.

The proposed modifications of the design procedures in prEN 1995-1-1 (2024) enable a more economical and reliable design of timber beam-columns prone to LTB.

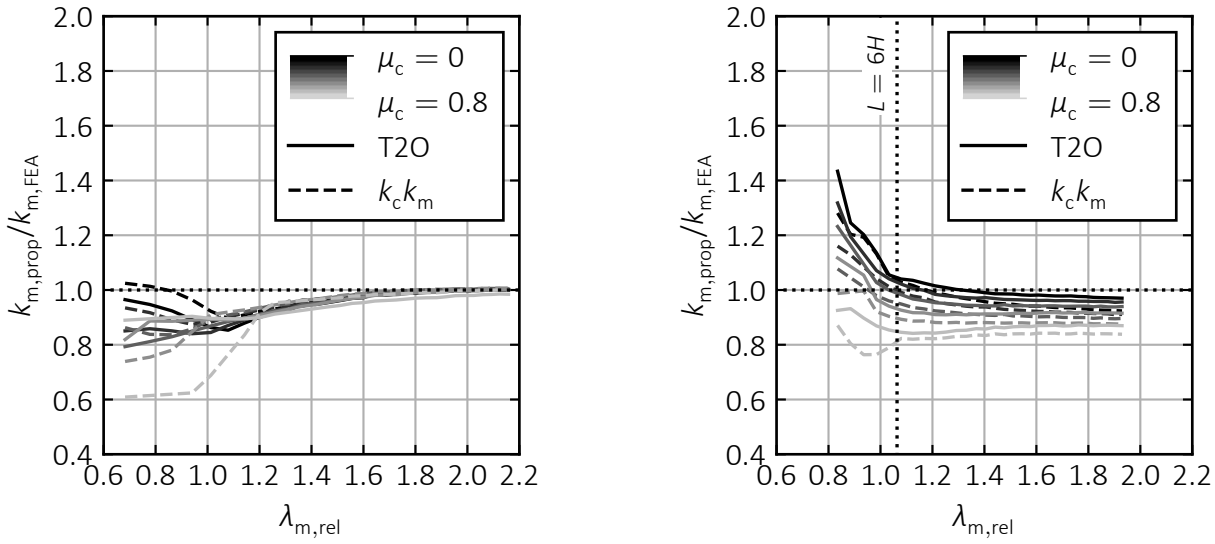

(a) Constant bending moment. *(b) Concentrated force at midspan.*

Figure 10. Ratio of the reduction factors by the design proposals in Section 7 to the reduction factors from FE analyses, $k_{m,prop}/k_{m,FEA}$, over the relative LTB slenderness $\lambda_{m,rel}$ for different utilisation ratios μ_c; GL 24h and $H/B = 8$.

8 Summary and outlook

This paper is based on the investigations described in *Töpler* & *Kuhlmann* (2023).

It is demonstrated analytically that the exponent 2 for considering compressive plasticizing in the N_x-$M_{y,2}$-interaction equation is on the safe side for common timber materials and that this interaction equation represents tensile failure for combined bending and compression, see Section 3.2. Subsequently, an analytical derivation of the nonlinear N_x-$M_{y,1}$-interaction for LTB of slender beam-columns is presented, see Section 3.3. Finally, a mechanical derivation of the k_m-method is described, see Section 3.4.

The results of 16 LTB tests on glulam beams made of GL 24h are discussed in Section 4, which confirmed the nonlinearity of the N_x-$M_{y,1}$-interaction for LTB.

An extensive numerical parameter study covering the reasonable member dimensions, different timber materials, and loading conditions for an in-depth analysis of the N_x-$M_{y,1}$-interaction at LTB is described in Section 5. It turned out that plate bending around the x axis at $H/B = 12$ increased the eigenvalues and the load-bearing capacities by up to 20%, see Section 5.2.1. For beams with $L/H < 6$ and subjected to shear forces, a pronounced cross-sectional warping due to shear stresses appeared and significantly reduced the load-bearing capacities, see Section 5.2.2. Generally, in-plane buckling occurred for $H/B = 1$ and LTB for $H/B \geq 2$. The FE results confirmed the non-linearity of the N_x-$M_{y,1}$-interaction for LTB. For significant shear forces, a reduction in shear stiffness due to shear plasticizing occurred, which reduced the load-bearing capacity by up to 20%. This was in line with the experimental results reported in *Töpler* & *Kuhlmann* (2023).

Based on the analytical, experimental, and numerical investigations, design proposals are presented in Section 7 that (i) consider the stiffness reduction due to compressive and shear plasticizing at LTB; (ii) contain mechanically derived equations for the k_m-method; and (iii) implement a limit criterion to account for the negative effect of shear warping on the edge bending stresses. But foremost, the nonlinear N_x-$M_{y,1}$-interaction for LTB from EN 1995-1-1 (2004) was confirmed.

In a subsequent publication, the shear verification for LTB of GL beams will be discussed.

9 Acknowledgements

The research project was supported by the German Federal Ministry for Economic Affairs and Climate Action on the basis of a decision of the German Bundestag (IGF project no. 21285 N). This support is gratefully acknowledged. We would like to thank the Forschungs- und Materialprüfanstalt (FMPA) of the Brandenburg University of Technology Cottbus-Senftenberg for conducting the experiments. We would also like to thank Schaffitzel Holzindustrie GmbH + Co. KG for providing the test specimens and Microtec Srl GmbH for providing the sorting data. Many thanks also to the members of the committee accompanying the project for the fruitful discussions and valuable comments.

10 References

Bell, K. & T. E. Eggen (2001). “Stability of timber beams and columns”. In: *International Association for Bridge and Structural Engineering (IABSE) Conference*. Lahti, Finland.

Blaß, H. J. (1987). “Design of timber columns”. In: *CIB-W18*. 20-2-2, Dublin, Ireland.

Buchanan, A. H.; K. C. Johns & B. Madsen (1985). “Column design methods for timber engineering”. In: *CIB-W18*. 18-2-1, Beit Oren, Israel.

DIN 1052 (2004). *Entwurf, Berechnung und Bemessung von Holzbauwerken – Allgemeine Bemessungsregeln und Bemessungsregeln für den Hochbau*. German Institute of Standardization (DIN), Berlin, Germany.

DIN 68364 (2003). *Kennwerte von Holzarten – Rohdichte, Elastizitätsmodul und Festigkeiten*. German Institute of Standardization (DIN), Berlin, Germany.

DIN EN 1995-1-1/NA (2013). *Nationaler Anhang – National festgelegte Parameter –Eurocode 5: Bemessung und Konstruktion von Holzbauten – Teil 1-1: Allgemeines – Allgemeine Regeln und Regeln für den Hochbau*. German Institute of Standardization (DIN), Berlin, Germany.

EN 14080 (2013). *Timber structures - Glued laminated timber and glued solid timber - Requirements*. European Committee for Standardization (CEN), Brussels, Belgium.

EN 1995-1-1 (2004). *Eurocode 5: Design of timber structures – Part 1-1: General – Common rules and rules for buildings*. European Committee for Standardization (CEN), Brussels, Belgium, with corrections and amendments + AC:2006 and A1:2008.

ETA-14/0354 (2018). *Beam BauBuche GL75*. Austria Institute of Construction Engineering (OIB), Vienna, Austria.

Heimeshoff, B. (1986). “Berechnung und Ausführung von Holzbauwerken”. In: *Ingenieur-Holzbau 86*. Leinfelden-Echterdingen, Germany.

Hörsting, O.-P. (2008). “Zum Tragverhalten druck- und biegebeanspruchter Holzbauteile”. Dissertation. Technische Universität Carolo-Wilhelmina zu Braunschweig, Braunschweig, Germany. DOI: https://doi.org/10.24355/dbbs.084-200807140200-0.

Leicester, R. H. (1988a). “Beam-column formulae for design codes”. In: *CIB-W18*. 21-2-2, Parksville, Vancouver Island, Canada.

Leicester, R. H. (1988b). “Format for buckling strength”. In: *CIB-W18*. 21-2-1, Parksville, Vancouver Island, Canada.

prEN 1995-1-1 (2024). *Eurocode 5 — Design of timber structures — Part 1-1: General rules and rules for buildings (Version 2a)*. CEN/TC 250/SC 5 N 2077. European Committee for Standardization (CEN): Brussels, Belgium.

Schänzlin, J.; G. Bosch & P. Hamm (2022). *k_c-method – consideration of creep deformations*. CEN/TC 250/SC 5/WG 3 N 354.

Schilling, S.; P. Palma & A. Frangi (2021). “Probabilistic description of the mechanical properties of glued laminated timber made from softwood”. In: *Proceedings of the 8th meeting of International Network on Timber Engineering Research (INTER)*. 54-12-4, online. DOI: https://doi.org/10.3929/ethz-b-000505371.

Taras, A. (2010). “Contribution to the development of consistent stability design rules for steel members”. Dissertation. Graz University of Technology, Graz, Austria. DOI: https://doi.org/10.3217/1smsn-1bq83.

Töpler, J. (2025). “Load-bearing capacity of imperfection-sensitive timber members under combined bending and compression”. in preparation. Dissertation. Institute of Structural Design, University of Stuttgart, Germany.

Töpler, J. & U. Kuhlmann (2022a). “Experimentelle und numerische Untersuchungen von Brettschichtholz aus Buchen-Furnierschichtholz (BauBuche)”. In: *Doktorandenkolloquium Holzbau Forschung und Praxis*. Stuttgart, Germany, pp. 131–139. DOI: http://dx.doi.org/10.18419/opus-12607.

Töpler, J. & U. Kuhlmann (2022b). “In-plane buckling of beech LVL columns”. In: *Proceedings of the 9th meeting of International Network on Timber Engineering Research (INTER)*. 55-2-1, Bad Aibling, Germany. DOI: http://dx.doi.org/10.18419/opus-12610.

Töpler, J. & U. Kuhlmann (2023). “Lateral torsional buckling of glulam beams”. In: *Proceedings of the 10th meeting of International Network on Timber Engineering Research (INTER)*. 56-12-6, Biel/Bienne, Switzerland. DOI: http://dx.doi.org/10.18419/opus-13593.

Töpler, J. & U. Kuhlmann (2024). *Optimierung des Ersatzstabverfahrens für biegedrillknickgefährdete Bauteile aus Holz unter Momenten-Normalkraft-Belastung*. Research report, IGF No. 21285 N. Institute of Structural Design, University of Stuttgart, Stuttgart, Germany.

van der Put, T. A. C. M. (1991). “Discussion of failure criterion for combined bending and compression”. In: *CIB-W18*. 24-6-1, Oxford, England.

Wilden, V.; B. Hoffmeister & M. Feldmann (2023). “Ein mechanisch konsistenter Ansatz für den Stabilitätsnachweis für Holztäger unter Druck und Biegung um die starke Achse”. In: *Bautechnik* 100.Sonderheft Holzbau, pp. 19–30. DOI: https://doi.org/10.1002/bate.202200073.

Zahn, J. J. (1986). “Design of wood members und combined load”. In: *Journal of Structural Engineering* 112.9, pp. 2109–2126. DOI: https://doi.org/10.1061/(ASCE)0733-9445(1986)112:9(2109).